A functional renormalization group for signal detection and stochastic ergodicity breaking

Journal of Statistical Mechanics: Theory and Experiment
An IOP and SISSA journal

PAPER: Classical statistical mechanics, equilibrium and non-equilibrium

A functional renormalization group for signal detection and stochastic ergodicity breaking

Harold Erbin[1,2,3], **Riccardo Finotello**[1,*], **Bio Wahabou Kpera**[1,4], **Vincent Lahoche**[1] and **Dine Ousmane Samary**[1,4]

[1] Université Paris-Saclay, CEA, LIST, Palaiseau, F-91120, France
[2] Center for Theoretical Physics, Massachusetts Institute of Technology, Cambridge, MA, 02139, United States of America
[3] NSF AI Institute for Artificial Intelligence and Fundamental Interactions, Cambridge, MA, 02139, United States of America
[4] Faculté des Sciences et Techniques (ICMPA-UNESCO Chair) Université d'Abomey-Calavi, Abomey-Calavi, 072 BP 50, Benin
E-mail: riccardo.finotello@cea.fr, erbin@mit.edu, wahaboukpera@gmail.com, vincent.lahoche@cea.fr and dine.ousmanesamary@cipma.uac.bj

Received 25 January 2024
Accepted for publication 24 June 2024
Published 2 August 2024

Online at stacks.iop.org/JSTAT/2024/083203
https://doi.org/10.1088/1742-5468/ad5c5c

Abstract. Signal detection is one of the main challenges in data science. As often happens in data analysis, the signal in the data may be corrupted by noise. There is a wide range of techniques that aim to extract the relevant degrees of freedom from data. However, some problems remain difficult. This is notably the case for signal detection in almost continuous spectra when the signal-to-noise ratio is small enough. This paper follows a recent bibliographic line, which tackles this issue with field-theoretical methods. Previous analysis focused on equilibrium Boltzmann distributions for an effective field representing the degrees of freedom of data. It was possible to establish a relation between signal detection and $\mathbb{Z}_2$-symmetry breaking. In this paper, we consider a stochastic field framework inspired by the so-called 'model A', and show that the ability to reach, or not reach, an equilibrium state is correlated with the shape of the dataset. In

*Author to whom any correspondence should be addressed.

particular, by studying the renormalization group of the model, we show that the weak ergodicity prescription is always broken for signals that are small enough, when the data distribution is close to the Marchenko–Pastur law. This, in particular, enables the definition of a detection threshold in the regime where the signal-to-noise ratio is small enough.

Keywords: functional renormalization group, Stochastic field theory, Signal detection, random matrix theory.

Contents

1. Introduction **2**

2. The model and associated path integral **7**
2.1. Technical preliminaries 7
2.2. The model and Martin–Siggia–Rose formalism 11

3. Functional renormalization group **12**
3.1. Functional renormalization in a nutshell 13
3.2. Local potential approximation 16
3.3. Scaling and dimensions 18

4. Numerical flow analysis and the signal track **19**
4.1. Numerical methodology 20
4.2. Results and comments 22
4.3. Exploring the phase space 24

5. Conclusion **27**

Acknowledgments **28**

References **28**

1. Introduction

In recent years, many authors have pointed out the connection between the renormalization group (RG) and data science—see, for instance [1–15] and references therein. This is not surprising, as for both techniques, the goal is the same: to extract large-scale regularities and relevant features for a system with interacting (i.e. highly correlated) degrees of freedom. Indeed, the RG aims to track a small number of relevant parameters ('couplings'), which describe the effective long-distance physics, in a quantum or statistical system involving a large number of interacting degrees of freedom (like a field theory). There are many incarnations of this idea: the most popular nowadays being the Wilsonian point of view [16]. In this realization, RG transformations look at partial

J. Stat. Mech. (2024) 083203

integration of fluctuations at the microscopic scale, that leave the long-distance physics unchanged but modify the effective couplings between infrared degrees of freedom. The basic incarnation of this strategy is Kadanoff's block spin construction where, at each step, the effective spin variables are locally replaced by their average. Due to its rather general scope, the RG finds applications in almost all physical domains, see [17] and references therein for a general overview of RG applications, and [18, 19] for a comprehensive presentation of concepts.

In some cases, the links between data science methods and the RG may look like a formal analogue rather than a guiding principle. Recently, the point of view seems to be evolving, and several authors have started to take the idea that a deeper connection exists between the two very seriously. Moreover, the idea that some problems inherent to big data analysis, and to artificial intelligence (AI) in general, can be approached as physical systems is starting to gain ground. One can mention, for instance, the series of papers [8–12] aiming to build an effective field theory model for artificial neural networks, and studying their properties by analyzing the RG. Complementary, works such as [20], enable the use of the exact RG as an optimal transport gradient flow, with interesting applications to neural network training. Other approaches focus on a comparison with so-called 'explainable' methods [21], such as principal component analysis (PCA) [5, 22–25]. This paper follows the bibliographic line of the authors [26–30] and is part of this dynamic. These works focus in particular on a problem where the current analysis methods often fail: signal detection in nearly continuous spectra[5] (see figure 1).

The idea behind this approach is based on the concept of universality. Totally noisy spectra indeed have a universal character, close, for instance, to properties of large-size Wishart matrices, whose spectra follow the Marchenko–Pastur (MP) law, see figure 2. Basically, the spectra observed for high-dimensional data are usually completely 'blind' to the real nature of the degrees of freedom involved in these statistics, whether it is the activity of biological neural networks [32], financial data [33], correlations between genes in DNA, and so on. Hence, the path proposed in [26–30] leads to the idea that the problem of signal detection can be equivalent to the RG study. We can then design an analogue statistical field theory model as follows. Suppose we are able, for a particular problem whose large-scale statistics are in the neighbourhood of a matrix universality class, to propose an effective field theory model exploiting the specific nature of the considered degrees of freedom. Furthermore, suppose that this field theory says something about the presence or absence of the signal. Hence, this same field theory must be able to give the same kind of answer for any data in the neighbourhood of the same universality class.

The usual example is an Ising-type model, for which one can easily build an effective field theory once the moments of orders 1 and 2 are fixed. The minimal model (in the sense of 'less structured': pioneer works on this topic of maximum entropy inference in physics are those of Jaynes [34, 35]) for this field theory is the one of maximum entropy, which takes the form of a Boltzmann law $\rho_{\rm eq}[\phi] \sim {\rm e}^{-\mathcal{S}[\phi]}$ for the field ϕ, with

[5] When only a few isolated spikes exist, detection is easy and general theorems exist, viewing the detection as a phase transition—the so-called Baik-Ben Arous-Péché' ('BBP') theorem, see [31].

J. Stat. Mech. (2024) 083203

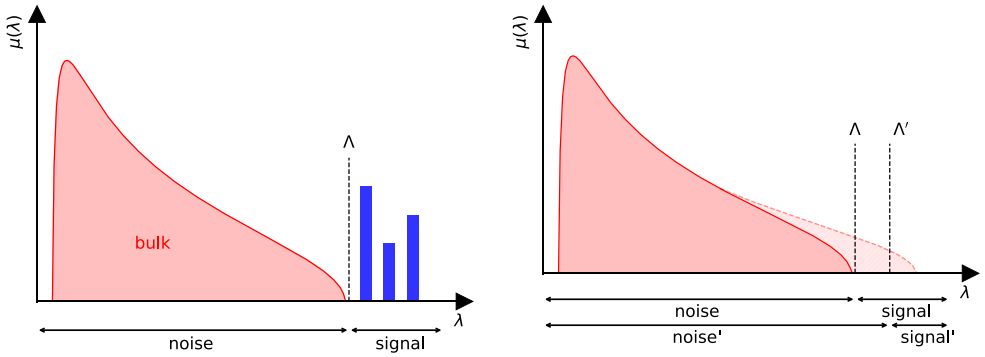

(a) Spectrum with localized spikes. (b) Spectrum with continuous deformation.

Figure 1. Depending on the nature of the underlying data, an empirical spectrum can exhibit some localized spikes (a) out of a bulk (i.e. noise, in red) made of delocalized eigenvectors (i.e. relevant information, in blue), in which case the cut-off Λ provides a clean separation between delocalized eigenvectors and localized ones. In the nearly continuous spectra (b), the position of the cut-off Λ is arbitrary, and the separation of the signal can become impossible.

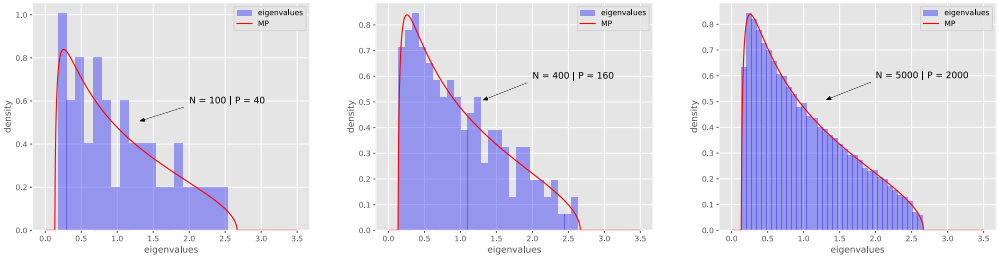

(a) $N = 100$, $P = 40$. (b) $N = 400$, $P = 160$. (c) $N = 5000$, $P = 2000$.

Figure 2. (a)–(c) Convergence towards the Marchenko–Pastur law for large-size $N \times P$ Wishart matrices ($P/N = 0.4$).

a non-trivial Gaussian measure such that the 2-point function G is identified with the covariance matrix $\mathcal{C}$ of the dataset (see also works in statistical inference, such as [36]). We thus proposed an effective field theory, general in scope, and unconventional in the construction of the RG due to the specific nature of the Gaussian kernel spectrum. This field theory describes an abstract type of matter filling a one-dimensional space, and whose interacting 2-point density spectrum is the data covariance matrix. See [30] for a general and comprehensive review of the state of the art of this approach. In summary, we can make the following empirical statements about RG analysis in the vicinity of the Marchenko–Pastur law (see figure 3):

- For purely noisy data, only local quartic and sextic couplings can be relevant to marginal in the large eigenvalue region (IR) domain. Moreover, there is a non-vanishing compact region around the Gaussian fixed point, where all trajectories end towards the $\mathbb{Z}_2$ symmetric phase;

J. Stat. Mech. (2024) 083203

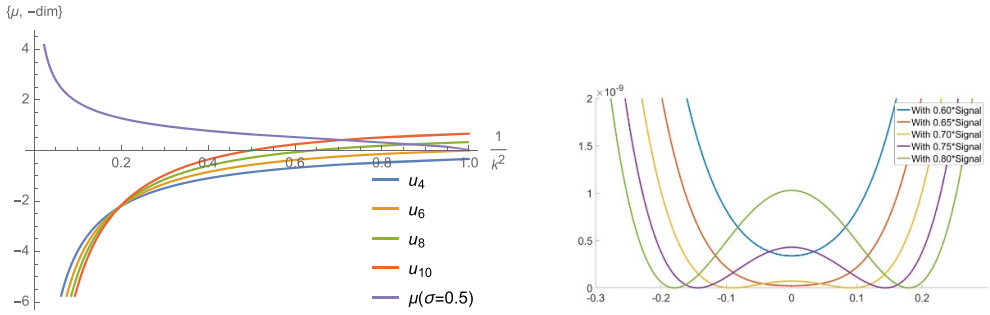

(a) Canonical dimensions. (b) IR effective potential.

Figure 3. The behaviour of the canonical dimensions (a) of local couplings (u_{2n}) of ϕ^{2n} interaction for the Marchenko–Pastur law and the shape of the effective potential in the deep IR (b), depending on the strength of the signal embedded in a random Wishart matrix. Reproduced with permission from [30].

- A strong enough signal makes the quartic and sextic local couplings irrelevant. Moreover, it induces a lack of symmetry restoration in the deep IR, for some trajectories which end continuously towards a broken phase. Hence, the strength of the signal plays the role of the inverse of the temperature $\beta = 1/T$ in the familiar physics of phase transitions.

These results seem to link the presence of a signal to macroscopic properties of the associated field theory. However, this approach focuses by construction, on an equilibrium distribution, of maximum entropy. In this paper, we propose to study the stability of this assumption regarding the presence of information in the spectrum, as the ratio of the signal to noise remains small enough. More precisely, we aim to establish a link between the stability of the maximal entropy distribution and the detection ability of the information merged in the noise. Note that mathematically, what we mean by not detectable is the presence of sufficiently localized eigenvectors in the spectrum.

The model we consider in this paper takes the form of a dissipative Langevin equation, reminiscent of the so-called *model A* [37] encountered in out-of-equilibrium statistical physics, and describing evolution of a real field with respect to a time variable t, such that the equilibrium distribution for the field variable $\phi(t)$ corresponds to the maximum entropy estimator $\rho_{\text{eq}}[\phi]$. This would incidentally not be the first occurrence of a stochastic model in the analysis of correlations of large data systems. In [38], for example, Langevin dynamics is considered to study Hebbian learning [39] and patterns of synaptic activity in many connected biological neurons and, in particular, to study the connection matrix in slow modes. In statistical physics, specifically in spin glass theories, a dynamical point of view gives a complementary insight into the study of metastable states appearing at large in these types of systems. The well-known Glauber model gives an example of such dynamics for a system subjected to the influence of a thermal bath inducing random transitions [40], and the so-called model A is nothing but a coarse-grained description of Glauber dynamics. More generally, the properties of

J. Stat. Mech. (2024) 083203

time evolution and the role of fluctuations near the transition temperature are important issues in the theory of phase transitions [41].

In these examples, however, time is always an external variable. But what about it in general? Can we associate an abstract temporal dimension to a set of data, to get a universal framework of Langevin-like dynamics? An interesting connection between temporality and statistics, known as the 'thermal time hypothesis' in the literature, was established in the 1990s [42]. The author points out the equivalence between the definition of a statistical equilibrium and the choice of a preferred time (i.e. a Hamiltonian flow), especially for covariant systems for which such a choice does not exist *a priori*. From this point of view, a clock is nothing other than a system in equilibrium with the studied system, running linearly with the parameter of the Hamiltonian flow. This point of view was generalized by Connes and Rovelli [43], who proved that, for quantum systems, a one-parameter group of automorphisms (identified as a time stream) exists, intrinsic to the von Neumann algebras, independently of the quantum state considered (this is a corollary of the Tomita–Takahashi theorem [44]). Obviously, in these cases, there is a notion of temporality at the beginning. For covariant systems, for example, the thermal time hypothesis only explains why, once a notion of equilibrium is fixed, a time stands out from the others and will tend to impose itself as a natural choice.

In our case, however, there is no notion of time at the beginning, and the question is: *can we think of a canonical notion of time hidden behind the distributions of big data correlations?* We do not answer that fundamental question in this article. We focus on a particular regime of non-equilibrium behaviour, such that the equilibrium distribution $\rho_{\rm eq}[\phi] \sim {\rm e}^{-\mathcal{S}[\phi]}$ is invariant to the notion of 'time' introduced in the article. Obviously, there is no single model of a stochastic equation that satisfies this condition, and we will keep things simple by considering a dissipative Langevin-type equation:

$$\frac{{\rm d}\phi}{{\rm d}t} = -\frac{\partial \mathcal{S}}{\partial \phi\,(t)} + \eta\,(t)\,, \tag{1.1}$$

where $\eta(t)$ denote some Gaussian noise, with zero mean and the delta-correlated 2-point function $\langle \eta(t)\eta(t')\rangle \propto \delta(t-t')$. Equation (1.1) is probably one of the simplest to describe a dissipative process decreasing the energy. It has been abundantly considered in the literature [37, 45]. Obviously, a safer approach would be to follow the strategy described in [28], and deduce this equation from a particular problem, whose correlation spectrum tends towards a large-scale universal law. In this way, we could still use the same universality argument to justify this model, whatever the microscopic reality of the problem under study. This is not the choice of this article, where we limit ourselves to motivating the choice of a stochastic approach, and reserve the underlying physical issues for a later work.

Once this framework is established, we will focus on the study of its equilibrium dynamics for which we will be able to write a path integral, and build an RG *á la Wilson* by partially integrating on the spectral degrees of freedom. Note that it would also be possible to integrate jointly on the temporal degrees of freedom [46–48]. However, we will not make this choice here, and the model presented in this article will be the subject of further studies. We will use the Wetterich–Morris functional formalism, which is more adapted to the non-perturbative analyses required for this type of theory [49–52].

J. Stat. Mech. (2024) 083203

The main results of this article regarding the signal detection issue in nearly continuous spectra can be summed up as follows:

- We assume, in the derivation of our effective field theory, that the system possesses non-translational invariance in time, and is in a large-time equilibrium dynamics regime;
- For a totally noisy spectrum, in the vicinity of the MP's universality class, we observe that the system almost never returns to equilibrium and the flow diverges at a finite scale, after a few RG steps (failure of the ergodic assumption);
- When the signal-to-noise ratio is low, the presence of a strong enough signal results in a sudden disappearance of divergences, at least for a compact region of the phase space around the Gaussian fixed point, no longer violating the assumption of a return to equilibrium;
- The boundary between the two domains is marked by a critical value β_c of the signal-to-noise ratio, which we are able to estimate.

In section 2 we define the model and conventions, and provide technical preliminaries. In section 3, we provide a short presentation of the Wetterich–Morris formalism in this specific context, to study the stochastic field theory in an equilibrium dynamics phase. We furthermore introduce the local potential approximation (LPA) for analyzing the RG equation near the phase transition. In section 4, we consider the previous formalism for spectra near the Marchenko–Pastur law, and we show that, universally, ergodicity is broken and equilibrium is (almost) never reached for small enough signals (domain coarsening phase). Furthermore, near the detection size (i.e. for the temperature β near the critical value β_c) a slowing down effect is observed and the correlation time becomes arbitrarily large. Finally, we conclude by enumerating some open questions that we plan to investigate in the future (section 5).

2. The model and associated path integral

This section provides the technical background underlying the study of this paper. In the first part, we provide a short review of the framework and of the state of the art in the domain. Next, we introduce the stochastic field theory model that we consider in the rest of this paper. Furthermore, assuming to work in the equilibrium dynamics regime, we use the Martin–Siggia–Rose (MSR) formalism to write the dynamics as a path integral. In the second part, we introduce the Wetterich–Morris equation and the LPA, allowing us to investigate it in a non-perturbative regime.

2.1. Technical preliminaries

As recalled in the introduction, standard PCA tools work well for spectra involving few discrete spikes isolated from the bulk. In that case, only a very small number of eigenvalues are representative of a large fraction of the total variance, materialized by

J. Stat. Mech. (2024) 083203

a gap in eigenvalues, for some $K = \Lambda$ in the fraction:

$$\zeta(K) \stackrel{\text{def}}{=\!=} \frac{\sum_{\mu=0}^{K} \lambda_\mu}{\operatorname{Tr} C}, \tag{2.1}$$

where C denotes the *covariance matrix* and $\{\lambda_\mu\}$ is the set of its eigenvalues. In practice, we focus on datasets defined by $N \times P$ matrices $X = \{X_{ai}\}$, where the indices a and i run along the sets $\{1, \ldots, P\}$ and $\{1, \ldots, N\}$, respectively. Basically, datasets are assumed to be large sets of large vectors. Assuming that the matrix X is suitably mean-shifted, the covariance C looks like a Wishart $N \times N$ matrix:

$$C = \frac{X^T X}{P}, \tag{2.2}$$

where T means standard transposition. Technically, since large variance contributions should dominate the spectrum, it is again convenient to work with the *correlation matrix*, whose entries are defined as:

$$\tilde{C}_{ij} = \frac{C_{ij}}{\sqrt{C_{ii} C_{jj}}}. \tag{2.3}$$

On the left of figure 1, we qualitatively illustrate the situation, where some discrete spikes capture a large fraction of the covariance matrix. In [30], we introduced the idea that the problem of distinguishing noisy from informational degrees of freedom for a nearly continuous spectrum near a random matrix universality class can be transposed to the RG study of an analogous field theory, describing an unconventional kind of matter filling an abstract space of dimension 1.

As recalled in the introduction, it is interesting to notice that the definition of this field theory does not depend on the specific nature of the data for which we aim to study the correlations. Indeed, since we focus on the vicinity of a universal spectrum of random matrices, any effective or analogue field theory able to represent correlations for a specific problem can represent correlations for all datasets in the vicinity of the same universality class, if its mathematical formulation is general enough. This is essentially the meaning of the universality class, and a reflection of the fact that spectra are blind to the 'microscopic' nature of the degrees of freedom that they describe. In this paper, we follow the working methodology of [30]. As we aim to establish a link between the properties of an effective field theory and signal detection, it is crucial in our numerical experiment to keep the spectra that we investigate under control and, in particular, the signal-to-noise ratio threshold. In practice, we have a parameter $T(\equiv \beta^{-1}) \in [0, 1]$, such that, for $T = 0$, X becomes a purely i.i.d[6]. random matrix of size $N \times P$, and the spectrum of $\tilde{C}(T = 0)$ goes towards MP law weakly as $N, P \to \infty$, keeping $P/N \stackrel{\text{def}}{=\!=} \alpha \geqslant 1$ fixed. In formulas, denoting x_i as the eigenvalues of $\tilde{C}$ for $T = 0$, we have [53]:

$$\mu_e(x) \stackrel{\text{def}}{=\!=} \frac{1}{N} \sum_{i=1}^{N} \delta(x - x_i) \to \mu_{\text{MP}}(x) = \frac{1}{2\pi\sigma^2} \frac{\sqrt{(x - \lambda_-)(\lambda_+ - x)}}{x\alpha} \mathbf{1}_{[\lambda_-, \lambda_+]}, \tag{2.4}$$

[6] I.e., the entries of the matrix are independent and identically distributed variables.

J. Stat. Mech. (2024) 083203

where $\lambda_\pm = (1 \pm \sqrt{\alpha})^2$, σ^2 is the variance of the random entries and $\mathbf{1}_{[\lambda_-,\lambda_+]}$ vanishes outside the domain $x \in [\lambda_-, \lambda_+]$. In the continuum limit, we replace discrete sums by integrals:

$$\frac{1}{N}\sum_i f(x_i) \to \int \mu_{\mathrm{MP}}(x)\, f(x)\, \mathrm{d}x. \tag{2.5}$$

In the rest of this paper we consider that such continuum approximation also holds for the experimental density spectra $\mu_{\mathrm{exp}}(x)$ for $T \neq 1$, which we assume to be an implicit consequence of the nearly continuous approximation on which we focus in this paper. Presuming to work in the vicinity of the MP law, the effective statistical field theory considered in [30] describes correlations for the scalar field $\phi(p) \in \mathbb{R}$ for $p \in \mathbb{R}$ playing the role of momenta. The energy spectrum p^2 is assumed to take N values, such that, in the continuum limit $N, P \to \infty$, they are distributed according to an (*a priori* unknown) continuous bounded distribution $\rho(p^2)$. The model is described by the probability density $\rho_{\mathrm{eq}}[\phi] := \mathrm{e}^{-\mathcal{S}[\phi]}/Z$, the partition function being:

$$Z = \int [\mathrm{d}\phi]\, \mathrm{e}^{-\frac{1}{2}\sum_p \phi(-p)\left(p^2+u_2\right)\phi(p) - U[\phi]}. \tag{2.6}$$

In the expression, $[\mathrm{d}\phi]$ denotes the path integral measure and the potential $U[\phi]$ corresponds to a 'local' field theory [26][7]

$$U[\phi] = N\sum_{n=2}^{K} \frac{u_{2n}}{N^n} \sum_{\{p_1,\cdots,p_{2n}\}} \delta\left(\sum_{i=1}^{2n} p_i\right) \prod_{i=1}^{2n} \phi(p_i). \tag{2.7}$$

As in standard field theory, we call the real constants $\{u_n\}$ the couplings, and u_2 the mass. Here, N is the size of the correlation matrix $\tilde{C}(T)$, the dependency being crucial for the large N limit to be well-defined. In contrast with standard statistical or quantum field theories, the bare action $\mathcal{S}$ is essentially unknown, but the correlation functions of the theory are fixed 'experimentally' using a data-driven approach (this is very similar to the approach of NN-QFT proposed in [10, 12]). Specifically, the 2-point function $G(p^2)$,

$$G\left(p^2\right) \overset{\mathrm{def}}{=\!=} \frac{1}{Z}\int [\mathrm{d}\phi]\, \mathrm{e}^{-\mathcal{S}[\phi]}\phi(p)\,\phi(-p), \tag{2.8}$$

which includes quantum corrections (Dyson's series) of the self-energy $\Sigma(p^2)$:

$$G\left(p^2\right) = \frac{1}{p^2+u_2} + \frac{1}{p^2+u_2}\Sigma\left(p^2\right)\frac{1}{p^2+u_2} + \cdots = \frac{1}{p^2+u_2-\Sigma\left(p^2\right)}, \tag{2.9}$$

is assumed to be equal, for each value of p, to an eigenvalue of the empirical correlation function $\tilde{C}(T)$. For the Gaussian model, i.e. $u_{2n} = 0\,\forall\, n > 1$, the correspondence shows

[7] Strictly speaking, there is no locality principle underlying this theory because there is no 'background space'. We define locality from the formal similarity with standard field theory in Fourier space.

J. Stat. Mech. (2024) 083203

that $1/(p^2+u_2)$ should be identified with some x_i, and the mass μ_2 corresponds to the inverse of the largest eigenvalue λ_+, assuming we translated the spectrum such that the smallest eigenvalue λ_- is zero. If the variable x is distributed according to some distribution $\mu_0(x)$, we call $\rho_0(p^2)$ the induced distribution for p^2 in the Gaussian limit. For $u_n \neq 0$, the propagator receives quantum corrections through the self-energy $\Sigma(p^2)$ and, in general, $\rho(p^2) \neq \rho_0(p^2)$. However, since we focus on the tail of the spectra, i.e. the region for $p^2 \ll 1$, we expect the derivative expansion and LPA to work well. Basically, we consider:

$$G\left(p^2\right) \approx \frac{1}{Zp^2+m^2}, \tag{2.10}$$

where $Z \overset{\text{def}}{=\!=} 1-\Sigma'(0)$ and $m^2 \overset{\text{def}}{=\!=} u_2-\Sigma(0)$. In this approximation, we can assume that p^2 is distributed according to $\rho_0(p^2)$. Furthermore, in the strict LPA, $Z=1$, as in [30], we explicitly check that this approximation indeed makes sense. Hence, we postulate that all quantum corrections are included in the effective mass m^2, and:

$$\rho\left(p^2\right) \approx \rho_0\left(p^2\right). \tag{2.11}$$

The properties of the LPA for this model, and especially the relation between $\mathbb{Z}_2$ symmetry breaking and the strength of the signal, were studied in [30] and references therein, and we recalled the main results in the introduction. In this paper, we suggest another point of view: we consider dynamical rather than equilibrium phase transitions. More specifically, we aim to study the relationship between the presence of a detectable signal and the existence of equilibrium dynamics. We recalled a first observation, a phase transition associated with the presence of a sufficiently strong signal, to which we can attach (at least formally) a critical temperature. This has been investigated for an equilibrium theory, but we have not discussed the conditions for the existence of this equilibrium, or more precisely its stability. However, out-of-equilibrium systems of this kind, associated with a system possessing different phases, exhibit a singular property known as *coarsening* or *phase ordering dynamics*. If we move abruptly from a high-temperature (ergodic) regime to a temperature T below the critical temperature T_{C}, the system is free to choose between several values of the order parameter, in different regions of the background space, and each region then evolves independently of the others, so that the system never returns to equilibrium. The different phases 'grow' as a function of time, with a scaling law $R(t)$, but the system remains self-similar at every instant [37]. This scale invariance also seems in line with what would be expected for a totally noisy signal, and it would not be surprising if the effective field theory describing the large-scale collective behaviour of the degrees of freedom associated with such a signal exhibited such invariance. We will see in the following that this is indeed the case for the effective kinetic theory model we will be proposing. More precisely, we will see that a totally noisy signal in the vicinity of the MP's universality class never allows a return to equilibrium, and the inverse of the critical temperature seems to cancel out at this limit $T_{\mathrm{C}}^{-1}=0$. When this noisy spectrum is corrupted by a sufficiently strong

J. Stat. Mech. (2024) 083203

signal (albeit within the signal/noise small enough limit), this critical temperature suddenly takes on a non-zero value. Physically, it is tempting to interpret the existence of a region of the phase space supporting the equilibrium assumption as the manifestation of a macroscopic order which, in turn, one would like to consider as relevant information.

2.2. The model and Martin–Siggia–Rose formalism

In the previous section, we motivated the analysis of a stochastic model describing a certain type of out-of-equilibrium process, suitably described by a Langevin equation of a particular type. Because of the requirement that equilibrium theory corresponds to the field theory 'in equilibrium' considered in [30], we state the following 'model A type' candidate [41] equation defined in Fourier space:

$$\boxed{\frac{\mathrm{d}}{\mathrm{d}t}\varphi\left(p,t\right)=-\left(p^{2}+m^{2}\right)\varphi\left(p,t\right)-\frac{\partial U\left[\varphi\right]}{\partial\varphi\left(-p,t\right)}+\eta\left(p,t\right),} \tag{2.12}$$

which describes the temporal evolution of the random field $\varphi(p,t)$, while keeping the notation $\phi\equiv\phi(p)$ for the equilibrium field variable. The white noise $\eta(p,t)$ is assumed to be Gaussian, with zero mean and variance:

$$\left\langle \eta\left(p,t\right)\eta\left(p',t'\right)\right\rangle =2\ T\ \delta_{p,-p'}\delta\left(t-t'\right), \tag{2.13}$$

where the notation $\langle X\rangle$ is the average over the normalized noise distribution $\mathrm{d}\mu(\eta)$:

$$\left\langle X\right\rangle \overset{\text{def}}{=\!=}\int\mathrm{d}\mu\left(\eta\right)X. \tag{2.14}$$

The parameter T identifies the temperature of equilibrium states, and we set $T=1$ in the rest of this paper (see [19]). The stochastic process described by equation (2.12) can be equivalently expressed in terms of the probability density $P(\varphi,t)[\mathrm{d}\varphi]$ for the field to be in the functional domain $[\varphi,\varphi+[\mathrm{d}\varphi]]$, starting from an initial condition at $t=0$. This density probability explicitly reads as:

$$P\left(\varphi,t\right)\overset{\text{def}}{=\!=}\left\langle \prod_{p}\delta\left(\varphi_{\eta}\left(p,t\right)-\varphi\left(p\right)\right)\right\rangle , \tag{2.15}$$

where $\varphi_\eta(p,t)$ is a formal solution of equation (2.12), for a given η[8]. Furthermore, it obeys a Fokker–Planck equation [19], whose stationary solutions are[9]

$$P_{\mathrm{eq}}\left[\phi\right]\equiv\rho_{\mathrm{eq}}\left[\phi\right]\propto\exp\left(-\frac{1}{2}\sum_{p}\phi\left(-p\right)\left(p^{2}+m^{2}\right)\phi\left(p\right)-U\left[\phi\right]\right)\equiv\exp\left(-\mathcal{S}\left[\phi\right]\right), \tag{2.16}$$

[8] Note that the solution is unique as soon as the initial conditions are fixed because the equation is first order with respect to time. The probability density is obviously normalized to 1, due to the normalization of $\mathrm{d}\mu(\eta)$.

[9] For $T\neq1$, the equation is replaced by $P_{\mathrm{eq}}[\phi]\sim\mathrm{e}^{-\mathcal{S}/T}$, and we indeed identify T as the temperature for equilibrium states, as soon as $\mathcal{S}$ is identified with the Hamiltonian.

J. Stat. Mech. (2024) 083203

which is also the expected probability density for late time. Indeed, introducing the 'wave function'[10] $\Psi \overset{\text{def}}{=\!=} \mathrm{e}^{\mathcal{S}/2} P$, we have $\dot{\Psi} = -\hat{H}\Phi$, with

$$\hat{H} \overset{\text{def}}{=\!=} \frac{1}{2}\left(-\frac{\partial}{\partial\varphi} + \frac{1}{2}\frac{\partial\mathcal{S}}{\partial\varphi}\right)\left(\frac{\partial}{\partial\varphi} + \frac{1}{2}\frac{\partial\mathcal{S}}{\partial\varphi}\right). \tag{2.17}$$

The fundamental state is such that $\hat{H}\Psi_0 = 0$, namely $\Psi_0 = \mathrm{e}^{-\mathcal{S}/2}$, which exists if, and only if, Ψ_0 is normalizable,

$$\langle\Psi_0|\Psi_0\rangle = \int [\mathrm{d}\phi]\, \mathrm{e}^{-\mathcal{S}[\phi]}. \tag{2.18}$$

In that case, we expect the system to return towards equilibrium:

$$\lim_{t\to+\infty} P(\phi, t) = P_{\text{eq}}[\phi]. \tag{2.19}$$

In the equilibrium dynamics regime, the MSR [45, 54] formalism allows the representation of information about correlations of the field at different times as a partition function defined by a path integral over two fields. This partition function $\mathcal{Z}[J]$ can be defined as follows:

$$\mathcal{Z}[J] \overset{\text{def}}{=\!=} \left\langle \mathrm{e}^{\int \mathrm{d}t \sum_p J(-p,t)\varphi(p,t)} \right\rangle, \tag{2.20}$$

which, according to the MSR strategy, can be rewritten as:

$$\mathcal{Z}\left[J, \tilde{J}\right] = \int [\mathrm{d}\varphi]\,[\mathrm{d}\tilde{\varphi}]\, \mathrm{e}^{-\mathcal{S}[\varphi,\tilde{\varphi}] + \int \mathrm{d}t \sum_p J(-p,t)\varphi(p,t) + \int \mathrm{d}t \sum_p \tilde{J}(-p,t)\tilde{\varphi}(p,t)}, \tag{2.21}$$

where we included a source term $\tilde{J}$ for the auxiliary field $\tilde{\varphi}$ as well. The MSR action is defined as:

$$\mathcal{S}[\varphi, \tilde{\varphi}] \overset{\text{def}}{=\!=} \int \mathrm{d}t \sum_p \left(\frac{\tilde{\varphi}(-p,t)\,\tilde{\varphi}(p,t)}{2} + \tilde{\varphi}(-p,t)\left(i\dot{\varphi}(p,t) + \frac{1}{2}\frac{\partial\mathcal{S}}{\partial\varphi(p,t)}\right)\right). \tag{2.22}$$

Notice that we use the Itô prescription for the computation of the path integral, imposing, in particular, $\theta(0) = 0$ for the Heaviside theta function involved in the computation of the average, equation (2.20), see [19]. In the literature, the auxiliary field is known as a *response field*, for reasons that we do not explain here, though the interested reader may consult [55].

3. Functional renormalization group

There are many incarnations of the original Wilson idea of the RG, but many of them are not suitable for non-perturbative analysis, like the Polchinski equation, even if they are

[10] The terminology makes sense in imaginary time.

J. Stat. Mech. (2024) 083203

formally accurate. Nowadays, the most powerful approach for non-perturbative aspects of the RG is the Wetterich–Morris formalism that we will use in this paper—for more details on this topic, the reader may consult the standard [56]. In the first subsection, we introduce this general formalism for the field theory that we constructed in the previous section. Let us mention right away that, in our case, the Wetterich–Morris equation cannot be solved exactly (as is often the case in physics[11]), and approximations will be necessary. We will describe them in the second subsection. More details on the functional RG in this context can be found in the recent [47, 48] of the same authors or the standard [17, 46, 57]. Some recent papers also cover the topic of the RG in and out-of-equilibrium stochastic process, see for instance [58, 59].

3.1. Functional renormalization in a nutshell

Let us consider a field theory whose partition function is given by the path integral:

$$Z = \int [\mathrm{d}\phi]\, \mathrm{e}^{-\mathcal{S}[\phi]}. \tag{3.1}$$

In the Wilsonian point of view for the RG, microscopic degrees of freedom are integrated out. The fundamental cut-off is rescaled at each step, to provide β-functions that describe how partial integration changes the couplings involved in the classical action. In the point of view proposed by Wetterich and Morris [56], however, the fundamental scale remains fixed, but a running parameter playing the role of an infrared cut-off suppresses large-scale contributions in the effective action of ultraviolet modes. This infrared cut-off is denoted by k, and we modify the classical action as

$$\mathcal{S}[\phi] \to \mathcal{S}[\phi] + \Delta\mathcal{S}_k[\phi], \tag{3.2}$$

where the *regulator* $\Delta\mathcal{S}_k[\phi]$, which is of degree 2 in the field ϕ looks formally as a momentum and scale-dependent mass term, designed to decouple long-range energy modes (with respect to the scale k). Explicitly, for a field theory in D dimensions ($x \in \mathbb{R}^D$, $\phi : \mathbb{R}^D \to \mathbb{R}$):

$$\Delta\mathcal{S}_k[\phi] \overset{\text{def}}{=\!=} \frac{1}{2}\int \mathrm{d}^D x \mathrm{d}^D y\, \phi(x)\, R_k(x-y)\, \phi(y). \tag{3.3}$$

A typical shape for (the Fourier transform of) the function $R_k(x-y)$ is shown in figure 4. In the figure, we also show the behaviour of the threshold function:

$$f_k\left(q^2\right) = \frac{\partial_q R_k\left(q^2\right)}{q^2 + R_k\left(q^2\right)} \tag{3.4}$$

where q denotes the momentum in Fourier space. The function f_k is the typical integrand involved in the flow equation, and we see that the regulator reduces the windows on momenta to a small domain around $q^2 \approx k^2$.

[11] This is essential. It is often pointed out that the solutions proposed in this framework are approximate, which is, however, a characteristic of physics, not of the Wetterich formalism.

J. Stat. Mech. (2024) 083203

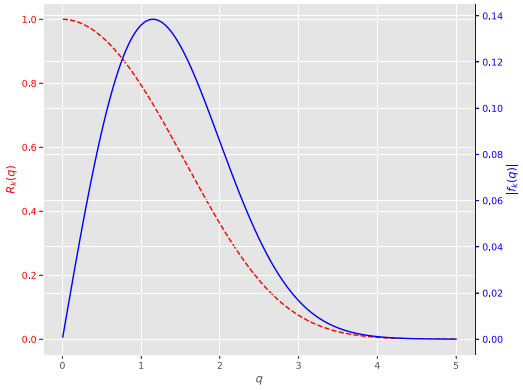

Figure 4. The behaviour of the threshold function for a typical regulator R_k (the dashed blue curve).

In practice, the regulator shape is designed such that:

- $R_k(q^2) \to 0$ as $|q| \to 0$, $k \to 0$, meaning that all the modes are integrated out in the deep infrared limit.
- $R_k(q^2) \to k^2$ as $|q|/k \to 0$, meaning that small energy modes decouple from long-distance physics.
- $R_k(q^2) \simeq 0$ as $|q|/k \gg 1$, meaning that high-energy modes remain unaffected by the regulator and are integrated out.

The Wetterich approach focuses on the effective average action Γ_k, which can be defined as the effective action for the ultraviolet modes (i.e. large with respect to the infrared scale k). This effective action is defined as the slightly modified Legendre transform of the free energy W_k:

$$\Gamma_k[M] + \Delta\mathcal{S}_k[M] = \int \mathrm{d}^D x\, J(x)\, M(x) - W_k[J], \tag{3.5}$$

where $J(x)$ is the source field, $M(x)$ is the classical field:

$$M(x) \stackrel{\text{def}}{=\!=} \frac{\delta W_k}{\delta J(x)}, \tag{3.6}$$

and the free energy W_k is defined as:

$$\mathrm{e}^{W_k[J]} \stackrel{\text{def}}{=\!=} \int [\mathrm{d}\phi]\, \mathrm{e}^{-\mathcal{S}[\phi] - \Delta\mathcal{S}_k[\phi] + \int \mathrm{d}^D x\, \phi(x) J(x)}. \tag{3.7}$$

Given the properties of the regulator, the effective average action Γ_k is a smooth interpolation between the fundamental classical action $\mathcal{S}$ and the full effective action Γ—that is, the true Legendre transform of the free energy when the regulator function is removed. For an ultraviolet cut-off $\Lambda \gg 1$, we thus have:

J. Stat. Mech. (2024) 083203

1. $\Gamma_{k=\Lambda} \simeq \mathcal{S}$ because $R_{k\to\Lambda} \sim \Lambda^2$ and quantum fluctuations are almost frozen;
2. $\Gamma_{k=0} \equiv \Gamma$ because $R_{k=0} = 0$ and all the fluctuations are integrated out.

The equation describing the variation of the interpolation Γ_k is the Wetterich–Morris equation, which explicitly reads as:

$$k\frac{\mathrm{d}}{\mathrm{d}k}\Gamma_k = \frac{1}{2}\int \mathrm{d}^D x \mathrm{d}^D y \left(k\frac{\mathrm{d}}{\mathrm{d}k}R_k\left(x-y\right)\right) G_k\left(x-y\right), \tag{3.8}$$

where the 2-point function G_k is the formal inverse of the 1PI 2-point function. In momenta:

$$G^{-1}\left(q^2\right) = \Gamma_k^{(2)}\left(q^2\right) + R_k\left(q^2\right), \tag{3.9}$$

where $\Gamma_k^{(2n)}$ denotes the $2n$-th order functional derivative of Γ_k with respect to the classical field M. The flow equation (3.8) is *exact*, but cannot be solved exactly in general, and approximations are required. Our aim in this paper is to study the RG corresponding to the MSR generating functional, equation (2.21). The method is described in recent works [46–48], and the reader may consult them and references therein for more details. The regulator has to be of the form:

$$\begin{aligned}\Delta\mathcal{S}_k \overset{\text{def}}{=\!=} \int \mathrm{d}t\mathrm{d}t' \sum_p r_k\left(p^2\right) \times \Big(& i\tilde{\varphi}\left(-p,t\right)\rho_k^{(1)}\left(t-t'\right)\varphi\left(p,t'\right) \\ &+\frac{1}{2}\tilde{\varphi}\left(-p,t\right)\rho_k^{(2)}\left(t-t'\right)\tilde{\varphi}\left(p,t'\right)\Big),\end{aligned} \tag{3.10}$$

where $r_k(p^2)$ is the Litim regulator [60] over the eigenvalues:

$$r_k\left(p^2\right) \overset{\text{def}}{=\!=} \left(k^2-p^2\right)\theta\left(k^2-p^2\right). \tag{3.11}$$

Time reversal symmetry of the MSR classical action corresponds to the field transformation:

$$\varphi'\left(p,t\right) \overset{\text{def}}{=\!=} \varphi\left(p,-t\right), \qquad \tilde{\varphi}'\left(p,t\right) \overset{\text{def}}{=\!=} \tilde{\varphi}\left(p,-t\right) + 2i\dot{\varphi}\left(p,-t\right). \tag{3.12}$$

The requirement that the modified action, equation (3.2), remains invariant under time reversal for all k implies:

$$\rho_k^{(1)}\left(t\right) - \rho_k^{(1)}\left(-t\right) + \dot{\rho}_k^{(2)}\left(-t\right) - \dot{\rho}_k^{(2)}\left(t\right) = 0. \tag{3.13}$$

In this paper we do not consider a coarse-graining over time (i.e. over frequencies), and we set $\rho_k^{(1)}(t) = 1 \Rightarrow \rho_k^{(2)}(t) \equiv 0$ because of equation(3.13). For a comparison between $\dot{\rho}_k^{(1)}(t) = 0$ vs $\dot{\rho}_k^{(1)}(t) \neq 0$ for a model close to the one considered in this paper, the reader may consult [47]. We expect that our approximation is as accurate as necessary for a proof of concept. In the next section, we discuss the LPA.

J. Stat. Mech. (2024) 083203

3.2. Local potential approximation

In [28], we considered the LPA for the equilibrium theory. In this section, we introduce the same formalism for the out-of-equilibrium field theory considered in this paper. Once again, more details about computations can be found in [47] of the same authors. In this approximation, we assume that the classical field has a macroscopic value χ for the deep IR component of the classical field $M(p)$ corresponding to the average value for the field φ:

$$M(p) = \sqrt{N\chi}\,\delta_{0,p}. \tag{3.14}$$

We furthermore assume the following ansatz for Γ_k:

$$\Gamma_k[\Xi] \overset{\text{def}}{=\!=} \Gamma_{k,\text{kin}}[\Xi] + \frac{1}{2}N\int \mathrm{d}t \sum_p i\,\tilde{\varpi}(-p,t)\,\frac{\partial U_k}{\partial M(p,t)}, \tag{3.15}$$

where $\Xi = (\tilde{\varpi}, M)$ collectively denotes the classical fields, i.e. the means values, respectively, for the response field $\tilde{\varphi}$ and the random field φ, and:

$$\Gamma_{k,\text{kin}}[\Xi] \overset{\text{def}}{=\!=} \int \mathrm{d}t \sum_p \left(Y_k \frac{\tilde{\varpi}(-p,t)\,\tilde{\varpi}(p,t)}{2} + i\,\tilde{\varpi}(-p,t)\left(Y_k \dot{M}(p,t) + Z_k p^2 M(p,t)\right)\right). \tag{3.16}$$

Since we focus on strict LPA, we furthermore assume (see [56]):

$$Y_k = Z_k = 1\,, \quad \forall k. \tag{3.17}$$

Furthermore, the equilibrium average action is ($m(p)$ here denotes the equilibrium classical field):

$$\begin{aligned}\Gamma_{k,\text{eq}}[m] &\equiv \frac{1}{2}\sum_p m(-p)\,p^2 m(p) + \frac{1}{2}U_k\left[m^2\right] \\ &= \frac{1}{2}\sum_p m(-p)\left(p^2 + \mu^2_{\text{eq}}(k)\right)m(p) + \mathcal{O}\left(m^4\right),\end{aligned} \tag{3.18}$$

and the physical mass $\mu^2_{\text{eq}}(k=0)$ is identified with the inverse of the largest eigenvalue of the empirical density spectra $\mu_{\text{exp}}(\beta)$ [30][12]. Furthermore, in the same reference, the authors checked, for the equilibrium theory in particular, that wave function renormalization is indeed a small correction, and we expect this approximation to make sense for the purpose of this paper. For the classical configuration, equation (3.14), we have:

$$\frac{1}{2}\frac{\partial U_k}{\partial M(p)} \to U_k'\left[M^2\right]M(p)\,, \tag{3.19}$$

[12] This is indeed a strong but crucial simplification of the LPA to store all the quantum fluctuations effects for the two-point function into the effective mass.

J. Stat. Mech. (2024) 083203

and $U_k[M^2]$ for a uniform macroscopic field is expected to admit a power expansion around some (running) minimum $\kappa(k)$:

$$U_k\left(M^2\right) = \frac{\mu_2\left(k\right)}{2}\left(\frac{M^2}{N} - \kappa\right)^2 + \frac{\mu_3\left(k\right)}{3}\left(\frac{M^2}{N} - \kappa\right)^3 + \cdots . \tag{3.20}$$

The flow equation for the effective potential U_k' can be derived from the Wetterich equation (3.8), imposing condition, equation (3.14), on both sides of the equation. From the truncation, we formally obtain:

$$\int \mathrm{d}t\, N \frac{\mathrm{d}}{\mathrm{d}s} U_k'[N\chi] = -i\frac{1}{\sqrt{N\chi}} \int \mathrm{d}t \sum_p \frac{\mathrm{d}}{\mathrm{d}s}\frac{\delta\Gamma_k}{\delta\tilde{\varpi}(p,t)} \equiv -\frac{1}{2}$$

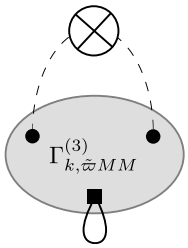

, (3.21)

where $\mathrm{d}s \overset{\text{def}}{=\!=} \mathrm{d}(\ln k)$. The last diagram corresponds to the right-hand side of the flow equation (3.8): the black dots and black squares represent, respectively, the fields M and $\tilde{\varpi}$, the solid self-loop is the sum and time integral over the variable of $\tilde{\varpi}(p,t)$, the dotted edge materializes the effective propagator G_k (equation (3.9)), and the crossed circle represents the regulator. The 3-point function $\Gamma_k^{(3)}$ can be easily computed:

$$\begin{aligned}\frac{\delta^3\Gamma_k}{\delta\tilde{\varpi}\left(p,t\right)\delta M\left(p_1,t_1\right)\delta M\left(p_2,t_2\right)} &= N\left(2U_k''\left[\delta_{p,p_1}\delta_{0,p_2} + \delta_{p,p_2}\delta_{0,p_1} + \delta_{p_1,p_2}\delta_{0,p}\right]\right.\\ &\quad \left. + 4\delta_{0,p}\delta_{0,p_1}\delta_{0,p_2}\chi N U_k'''\right)\\ &\quad \times \sqrt{N\chi}\delta\left(t-t_1\right)\delta\left(t-t_2\right).\end{aligned} \tag{3.22}$$

It is convenient to introduce the potential $\mathcal{U}_k$ such that:

$$\mathcal{U}_k\left[\chi\right] \overset{\text{def}}{=\!=} U_k\left[M^2 = N\chi\right]. \tag{3.23}$$

Hence, working in Fourier space, and because of the integral[13]:

$$\int_{-\infty}^{+\infty}\frac{\mathrm{d}\omega}{2\pi}\frac{1}{\left(i\omega + f\left(x\right)\right)^2\left(-i\omega + f\left(x\right)\right)} = \frac{1}{4}\frac{1}{\left(f\left(x\right)\right)^2}, \tag{3.24}$$

the flow equation for $\mathcal{U}_k'[\chi]$ reads explicitly reads:

$$\frac{\mathrm{d}}{\mathrm{d}s}\mathcal{U}_k'\left[\chi\right] = -2\frac{3\mathcal{U}_k''\left[\chi\right] + 2\chi\mathcal{U}_k'''\left[\chi\right]}{\left(k^2+\mu^2\right)^2}k^2\left(\int_0^k \mathrm{d}p\, p\,\rho\left(p^2\right)\right), \tag{3.25}$$

[13] It comes directly from residue theorem, assuming the function $f(x)$ does not vanish.

J. Stat. Mech. (2024) 083203

where we used the explicit expression for the derivative of the Litim regulator:

$$\frac{\mathrm{d}}{\mathrm{d}s} r_k\left(p^2\right) = 2k^2\theta\left(k^2 - p^2\right), \tag{3.26}$$

and the effective mass μ^2 is:

$$\mu^2 \overset{\text{def}}{=\!=} \mathcal{U}_k'\left[\chi\right] + 2\chi\mathcal{U}_k''\left[\chi\right]. \tag{3.27}$$

Furthermore, we replace the discrete sum over p by an integral, taking the continuous limit for the density spectrum:

$$\frac{1}{N}\sum_p \theta\left(k^2 - p^2\right) \to 4\left(\int_0^k \mathrm{d}p\, p\, \rho\left(p^2\right)\right). \tag{3.28}$$

3.3. Scaling and dimensions

For a power-law distribution $\rho(p^2) \sim (p^2)^\delta$, as is the case for the standard field theory[14], the loop integral in equation (3.25) behaves as $k^{2\delta+2}$. The explicit dependency on k can be cancelled on both sides of the flow equation, working with dimensionless quantities. Specifically, this allows one to take into account the rescaling of the fundamental scale after each partial integration, to keep the large-scale physics unchanged. In our case, however, the distribution is not a power law, and the integral in equation (3.25) does not behave as such. In that case, we cannot discard the explicit dependency on k. As pointed out in [28], the best compromise is to move this dependency to the level of the linear term, that we usually call the *canonical dimension* in the RG literature. Hence, according to [28], we introduce a new parameter τ, defined such that:

$$\mathrm{d}\tau \overset{\text{def}}{=\!=} \mathrm{d}\left[\ln\left(\int_0^k \mathrm{d}p\, p\, \rho\left(p^2\right)\right)\right]. \tag{3.29}$$

For a power-law distribution obviously, $\mathrm{d}\tau \propto \mathrm{d}\ln k$. Since the eigenvalues p^2 have to scale as μ^2, it is convenient to introduce the *dimensionless effective mass*:

$$\bar{\mu}^2 \overset{\text{def}}{=\!=} k^{-2}\mu^2. \tag{3.30}$$

We introduce the notation:

$$\dot{X} \overset{\text{def}}{=\!=} \frac{\mathrm{d}X}{\mathrm{d}\tau}. \tag{3.31}$$

for the τ derivative, and we denote as $\dim_\tau(X)$ the canonical dimension (i.e. the opposite of the linear term in the flow equation for X). Since the flow equation for μ^2 has to be multiplied by $\dot{s}$ to express the flow in the τ variable, the canonical dimension for μ^2 is:

$$\dim_\tau\left(\mu^2\right) \overset{\text{def}}{=\!=} \dim_\tau\left(\mathcal{U}_k'\right) = 2\dot{s}. \tag{3.32}$$

[14] For a field theory over $\mathbb{R}^d$, we have $\rho(p^2) \sim (p^2)^{\frac{d-2}{2}}$.

J. Stat. Mech. (2024) 083203

Henceforth, we define as $\bar{X}$ the dimensionless version of the quantity X. Using the τ parameter, the flow equation for U'_k (3.25) becomes:

$$\dot{\mathcal{U}}'_k[\chi] = -2k^2 \frac{3\mathcal{U}''_k[\chi] + 2\chi\mathcal{U}'''_k[\chi]}{(1+\bar{\mu}^2)^2}\left(\frac{\rho(k^2)}{k^2}\dot{s}^2\right). \tag{3.33}$$

To derive the flow equations for dimensionless couplings, it is convenient to work with a flow equation with fixed $\bar{\chi}$. The flow equation (3.25) is, however, written at a fixed χ. To convert one into the other, let us observe that:

$$\dot{\mathcal{U}}'_k[\chi] = k^2\left[\dot{\bar{\mathcal{U}}}'_k[\bar{\chi}] + \dim_\tau(\mathcal{U}'_k)\,\bar{\mathcal{U}}'_k[\bar{\chi}] - \dim_\tau(\chi)\,\bar{\chi}\bar{\mathcal{U}}''_k[\bar{\chi}]\right]. \tag{3.34}$$

The dimension of $\dim_\tau(\mathcal{U}'_k)$ has been computed in equation (3.32). From the flow equation (3.33), we define:

$$\bar{\mathcal{U}}''_k \overset{\text{def}}{=\!=} \mathcal{U}''_k \frac{\rho(k^2)}{k^2}(\dot{s})^2. \tag{3.35}$$

Obviously, $\chi\mathcal{U}'''_k$ and $\mathcal{U}''_k$ must have the same dimension, and the dimension of the field χ can be computed from equations (3.35) and (3.32):

$$\chi \overset{\text{def}}{=\!=} \left(\rho(k^2)\,\dot{s}^2\right)\bar{\chi}, \tag{3.36}$$

leading to:

$$\dim_\tau(\chi) = \dot{s}\frac{\mathrm{d}}{\mathrm{d}s}\ln\left(\rho(k^2)\,\dot{s}^2\right). \tag{3.37}$$

Finally, the flow equation for the dimensionless potential explicitly reads:

$$\boxed{\dot{\bar{\mathcal{U}}}'_k[\bar{\chi}] = -\dim_\tau(\mathcal{U}'_k)\bar{\mathcal{U}}'_k[\bar{\chi}] + \dim_\tau(\chi)\,\bar{\chi}\bar{\mathcal{U}}''_k[\bar{\chi}] - 2\frac{3\bar{\mathcal{U}}''_k[\bar{\chi}] + 2\bar{\chi}\bar{\mathcal{U}}'''_k[\bar{\chi}]}{(1+\bar{\mu}^2)^2}.} \tag{3.38}$$

This equation provides, in the LPA approximation, the full behaviour of the RG. As the formalism has been introduced, in the next sections we will study the RG flow for slightly deformed spectra around MP law.

Remark 1. According to the discussion in section 2.1, in equation (2.11), the distribution $\rho(p^2)$ is assumed to be equal to the distribution $\rho_0(p^2)$ for the Gaussian theory.

4. Numerical flow analysis and the signal track

This section aims to explore the behaviour of the RG for the theory described in the previous section (equation (3.38)). We start by studying the case of a totally noisy spectrum, that is, the analytical MP distribution. We then investigate the qualitative changes in the behaviour of the RG as a signal disturbs the noise matrix.

J. Stat. Mech. (2024) 083203

4.1. Numerical methodology

To simulate the flow equation (3.38), we use the Python package `py-pde` [61]. It enables the efficient simulation of partial differential equations of the general form

$$\dot{u}\left(\mathbf{x},t\right)=\mathcal{D}\left[u\left(\mathbf{x},t\right)\right]+\eta\left(u,\mathbf{x},t\right), \tag{4.1}$$

where $\mathcal{D}$ is a (generically non-linear) differential operator, $\dot{u}$ is the usual 'time' derivative and η is a noise term (in our case $\eta\equiv 0$).

As we are interested in the universality class of the MP distribution, we first focus on its analytic form, equation (2.4). We inverse it to obtain the functional form of the momenta $\rho(p^2)$ of the field theory (see figure 5):

$$\rho\left(p^2\right)=\mu_{\mathrm{MP}}\left(\frac{1}{p}\right)\frac{1}{p^2}. \tag{4.2}$$

We successively translate it such that $\rho(0)=0$. We then consider several empirical realizations to follow the deformation from the theoretical distribution. We consider a noisy signal given by the definition, equation (2.2), where the entries of the matrix X are independent and identically distributed (i.i.d.), with zero mean and unit variance. In the large N, $P\to\infty$ limit, but such that $P/N\overset{\mathrm{def}}{=\!=}\alpha<\infty$, the spectrum of C approximates the MP distribution defined by equation (2.4)—see also figure 2. To deform the spectrum of the universal class, we build a fixed-rank matrix S, added on top of the purely random matrix X. Specifically, we build an empirical matrix $Y\in\mathbb{R}^{N\times P}$ such that[15]:

$$Y=Z+\beta S, \tag{4.3}$$

where $Y=(y_{ij})_{i\in[1,N],j\in[1,P]}$ for $y_{ij}\sim\mathcal{N}(0,1)$, and $\beta\in[0,0.5]$ in these simulations. The signal matrix S represents the added signal. In the investigations carried out in [28, 30], the authors considered the spectrum of a correctly normalized image to materialize this signal. Here, we adopt a different strategy, which allows us to maintain even greater control over the experimental parameters. We build two rectangular matrices

$$U=(u_{ir})_{i\in[1,N],r\in[1,R]}\qquad\text{and}\qquad V=(v_{rj})_{r\in[1,R],j\in[1,P]} \tag{4.4}$$

for a fixed choice of $R<N,P$, such that $u_{ir}\sim\mathcal{N}(0,1)$ and $v_{rj}\sim\mathcal{N}(0,1)$. We then consider the product

$$S\overset{\mathrm{def}}{=\!=}\frac{UV}{\sqrt{R}} \tag{4.5}$$

[15] Notice the slight change of notation w.r.t. section 2.1, in order to conform to the standard literature in data analysis. All definitions can be recovered by either transposing the matrix X in the previous sections, or by inversing $P\longleftrightarrow N$.

J. Stat. Mech. (2024) 083203

as the definition of the signal matrix. The covariance matrix has the usual definition (row-wise variables):

$$C \overset{\text{def}}{=\!=} \frac{Y^T Y}{N}. \tag{4.6}$$

We rely on the interpolation of the (inverse) spectrum of the eigenvalues of C for the subsequent steps. Specifically, we fit a smoothed second-degree polynomial to the density histogram of the eigenvalues/momenta, using a B-spline representation of the curve. Integrations were carried out using the quadrature technique, while differentiation uses central differences to minimize the error.

For our numerical investigations, we set $N = 10^4$, $P = 8 \times 10^3$ and $R = 2500$. Moreover, we set the general initial condition

$$\bar{\mathcal{U}}_{k=0}[\bar{\chi}] = \bar{\mu}_1 \bar{\chi} + \frac{1}{2}\bar{\mu}_2 \bar{\chi}^2 + \frac{1}{3}\bar{\mu}_3 \bar{\chi}^3 + \frac{1}{4}\bar{\mu}_4 \bar{\chi}^4 \tag{4.7}$$

on the effective potential.

The simulation of the dynamic equation (3.38) has been carried out in a frequency domain centred on the low momentum scale of the underlying MP distribution. That is, we chose $k \in [k_-, k_+]$ in $\tau = \tau(k)$ (see equation (3.29)) such that:

$$k_\pm = \frac{1}{\lambda_+ \mp a}, \tag{4.8}$$

where λ_+ is defined in equation (2.4), and $a = 0.35$ in the simulations presented in this article. We set the simulation on a grid of 10^3 points in the interval $\bar{\chi} \in [0, 1]$.

At least as far as the 2-point function is concerned, the considered field theory is defined in the IR by construction (we have the exact function, including all quantum corrections—see equation (2.9)). This contrasts with the usual situation in field theory, where we define a microscopic theory whose large-scale effects are studied by the RG; here, our definition of microscopic theory is based solely on the approximation (LPA) used to describe the RG flow. For this reason, the microscopic theory should not be considered as realistic, in the sense that it does not reflect the reality of the microscopic degrees of freedom associated with the spectrum under consideration. It is only a projection of the actual theory, describing at a large distance the collective behaviour of these degrees of freedom. Our experimental approach reflects this reality, and unlike standard approaches, we choose (which makes sense for the approximation considered) to initiate the flow in the IR region by inducing the theory in the UV region. Although this approach is paradoxical from the point of view of the very meaning of the RG (a semigroup), it is not totally exotic either. It is, for example, the point of view adopted in the literature devoted to the problem of 'asymptotic safety' in quantum gravity [62], aiming to prove that quantum gravity is well-defined in the UV region, even if it is not (perturbatively) just renormalizable.

J. Stat. Mech. (2024) 083203

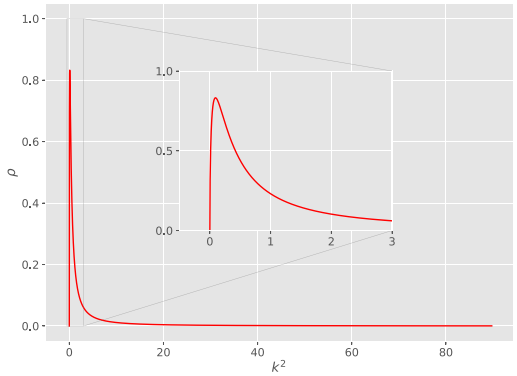

Figure 5. The typical shape of $\rho(p^2)$ for MP law. Note that we labelled the abscissa variables with k^2, the renormalization group scale.

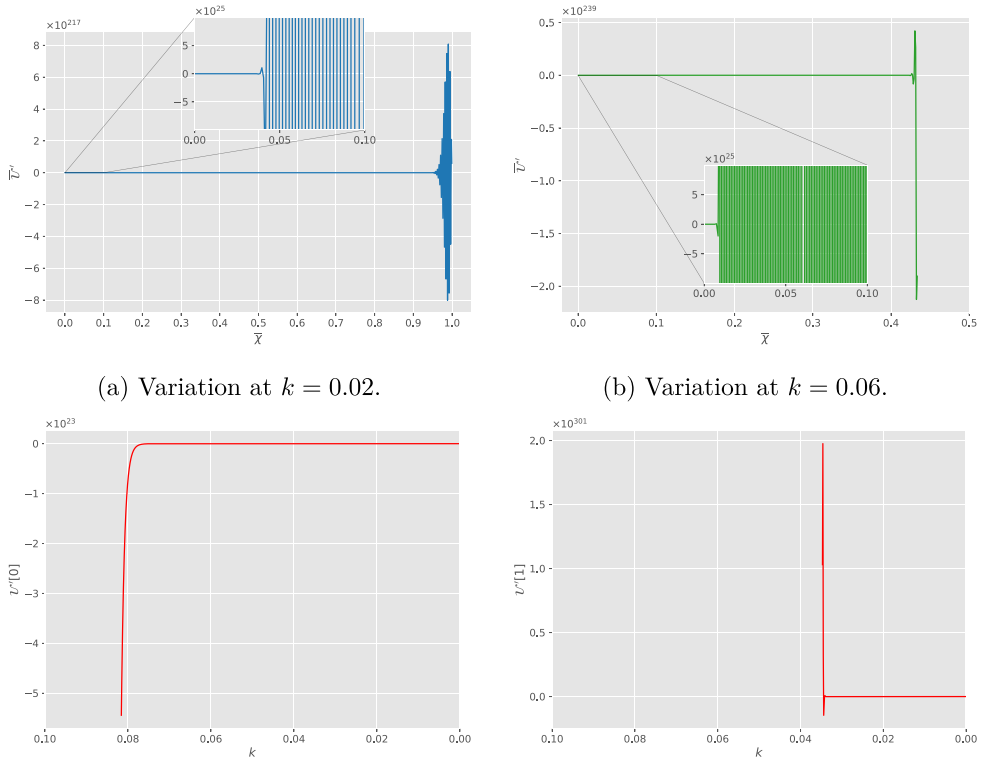

(a) Variation at $k = 0.02$.

(b) Variation at $k = 0.06$.

(c) Back-evolution of $\overline{\mathcal{U}}'[0]$.

(d) Back-evolution of $\overline{\mathcal{U}}'[1]$.

Figure 6. Typical variations of the potential (see (a) and (b)) and its back-evolution for the analytical MP law (see (c) and (d)). The initial conditions are the following: $\bar{\mu}_1 = \bar{\mu}_3 = \bar{\mu}_4 = 0.0$, $\bar{\mu}_2 = 1.0$. Arbitrary large and rapid oscillations are observed for the back-evolved potential, after some RG steps.

4.2. Results and comments

First, we consider the case of the MP spectrum. The corresponding ρ's shape is pictured in figures 5 and 6 and shows the typical behaviour of the back-evolution of the effective potential, with general initial conditions, equation (4.7).

J. Stat. Mech. (2024) 083203

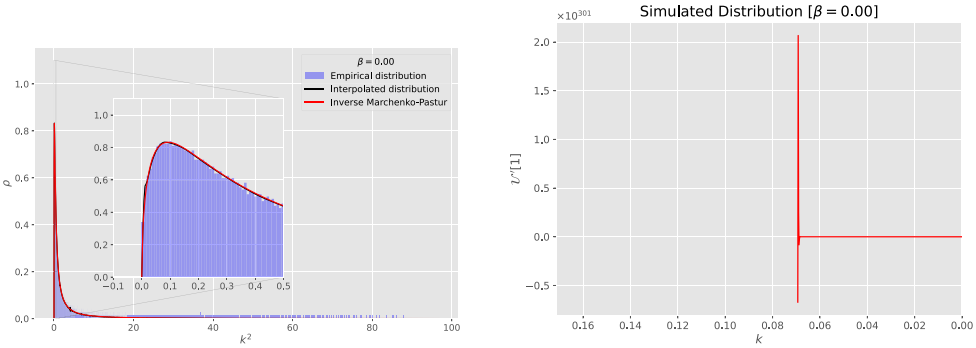

(a) Noisy ($\beta = 0$) empirical distribution.

(b) RG flow for $\beta = 0$.

Figure 7. The behaviour of the RG flow (b) in the case of the empirical distribution for $\beta = 0$ (a) is extremely similar to that obtained from the analytical MP law. The absence of values for $k \gtrsim 0.07$ signals the divergence of the values in the Python simulation.

Recall that, asymptotically in the IR, the power counting for the MP law reduces to that of a three-dimensional field theory, and that all interactions higher than sextic are irrelevant (see figure 3). The behaviour we observe is reminiscent of that found in classical models of disordered systems, such as p-spin models, whose functional RG has recently been considered [47, 48] in a temporal approach that is equivalent to that considered in this article. The authors observed the same type of divergence at finite k, which can be physically interpreted as the failure of the assumption that the system is in equilibrium dynamics. Indeed, this assumption is implicitly made in the construction of the MSR path integral, equation (2.21), because we took the origin of time for $t = -\infty$; due to the expected time translation invariance and because of the time reversal symmetry, the system is then assumed to be arbitrary close to equilibrium for any finite time. In the two previous references, the authors specifically confronted these assumptions, and showed that finite time singularities are truly related to a breakdown of the time reversal symmetry and time translation invariance (focusing on the breakdown of the underlying supersymmetry in [48] and through a 2PI formulation in [47]). Hence, in this model, we recover what we could expect from previous investigations: the system fails to reach equilibrium for general initial conditions in the deep IR[16].

It is also worth noting, for the following discussion, that these conclusions are not specific to the $P, N \to \infty$ limit. They remain true even when these parameters are finite, provided they are sufficiently large. Figure 7 illustrates this point, and the parameter β set to zero means the no-signal limit (see the convention given in the introduction, though this point will be clarified shortly). Once again, we recover the same phenomena: a finite scale divergence reminiscent of a weak ergodicity breaking.

Figure 8 shows some results for different values of the parameter β. On the left, we can see the empirical distribution for a given draw of Z, and on the right we show

[16] We could say for *almost all* initial conditions. It is indeed possible that the situation is different for some of them, as we saw in [47] (and references therein). However, we have not yet been able to identify any such conditions.

J. Stat. Mech. (2024) 083203

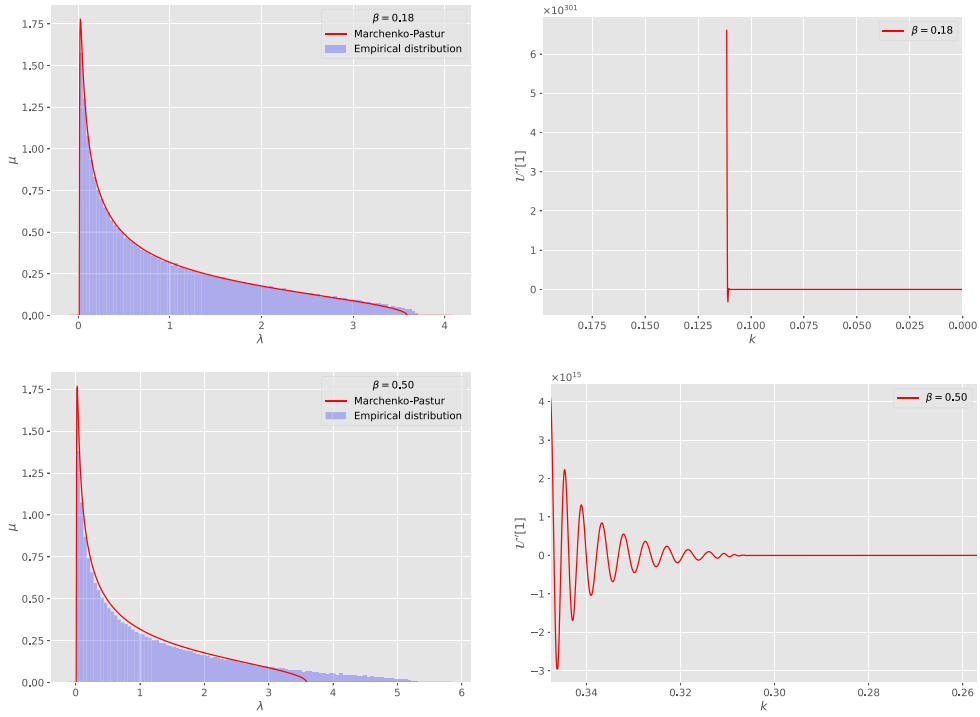

(a) Simulated empirical distribution. (b) RG flow.

Figure 8. The empirical spectrum with an increased signal level (a), and the corresponding back-evolution of the derivative of the potential at the (arbitrary) value $\bar{\chi} = 1$ (b).

the corresponding RG flow (with the same initialization as in figure 6). As long as β remains small, the results remain (qualitatively) those obtained previously for a purely noisy signal; there is, however, a slight delay in the explosion of the RG flow. When β is large enough, the behaviour of the RG flow is very different. Although the potential takes large absolute values, it does not seem to diverge, and its derivative also remains regular. Thus, our initial hypothesis seems to be confirmed: *a sufficiently large signal favours a return to equilibrium*, or at least does not reject this hypothesis, which is central to the construction of the MSR partition function. This qualitative change in the behaviour of the flow can be used to define a signal detectability threshold.

4.3. Exploring the phase space

Next, we choose a more convenient representation of the initial conditions in the IR, based on a single parameter that we will identify (after redefining the fields) as the (renormalized) temperature T:

$$\bar{\mu}_1 = \frac{T - T_0}{T}, \qquad \bar{\mu}_{n>1} = T^{n-1}. \tag{4.9}$$

J. Stat. Mech. (2024) 083203

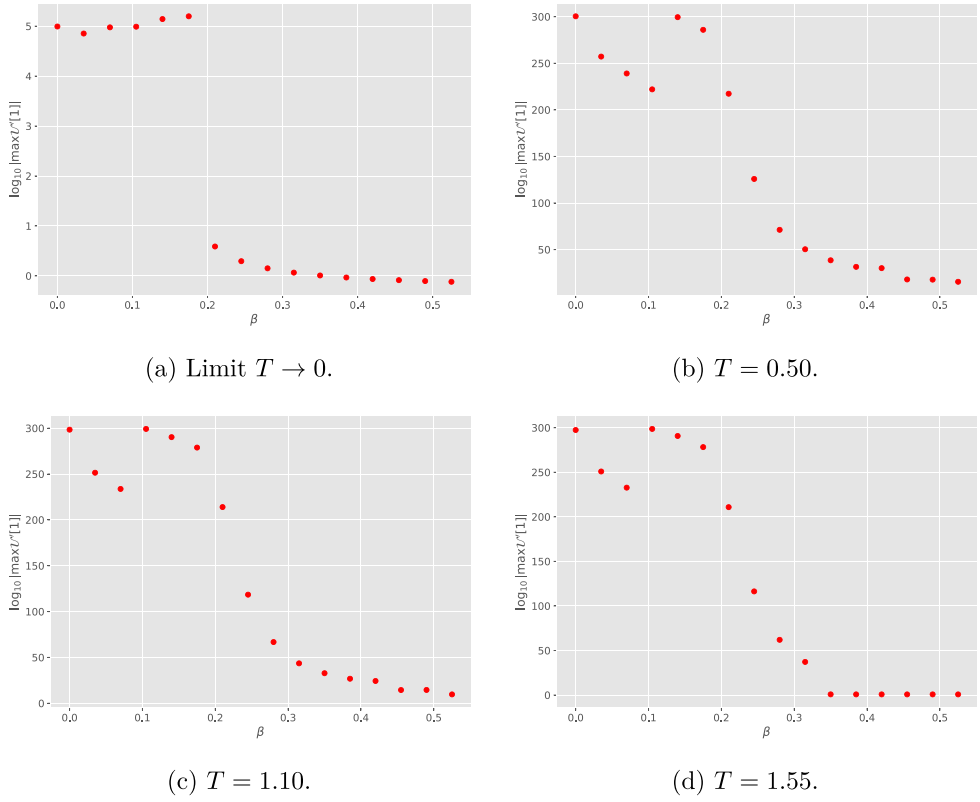

(a) Limit $T \to 0$. (b) $T = 0.50$.

(c) $T = 1.10$. (d) $T = 1.55$.

Figure 9. The behaviour of the (suitably normalized) absolute value for the maximum of the derivative of the potential at the point 1 with respect to β (a), and for different temperatures (b)–(d).

In this parametrization, the temperature T_0 is arbitrary, and we set $T_0 = 0.5$ as a 'test' value in the experiments (in this scenario, averaged over ten different realizations each). In figure 9, we plot the logarithm of the absolute value of the maximum of the derivative of the potential as a function of the value of β, for different temperatures. We can clearly identify a transition between two regimes, around the value $\beta_c \simeq 0.2$. Notice that this value does not seem to depend significantly on the T_0 value as well as on the value of $\bar{\chi}$ selected for the simulation: we were able to verify the statement numerically. It is worth noting that, although we had identified the existence of a critical β_c value for signal detection in our previous work [30], we had not yet been able to estimate it: indeed, we were able to show the occurrence of a symmetry-breaking mechanism as a result of the addition of signal to a normal background, though the value of the critical β_c could not be determined. This translated to a shrinkage of the domain of initial conditions leading to the symmetric phase, which provided a good, though insufficient, qualitative representation of the signal-to-noise ratio.

Finally, let us point out that while the figures appear similar for different temperatures, the $T \to 0$ limit is singular, and the transition to the critical value β_c seems more abrupt. This limit would physically correspond to the case of a totally uncorrelated noise; this phenomenon deserves to be completed by a finer physical analysis of the

J. Stat. Mech. (2024) 083203

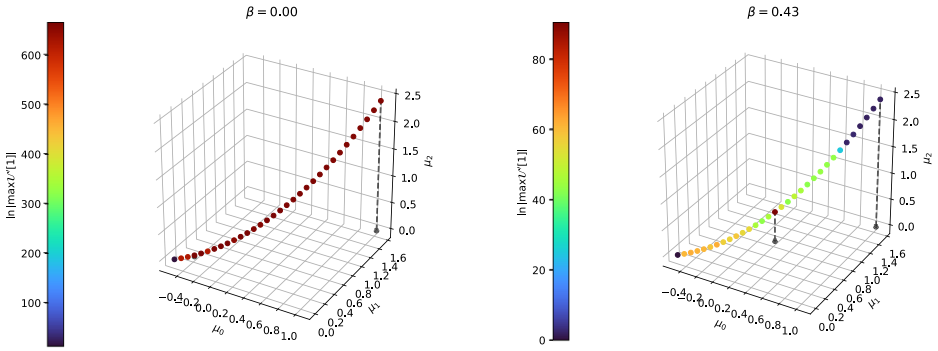

(a) Phase diagram at $\beta = 0.00$.

(b) Phase diagram at $\beta = 0.43$.

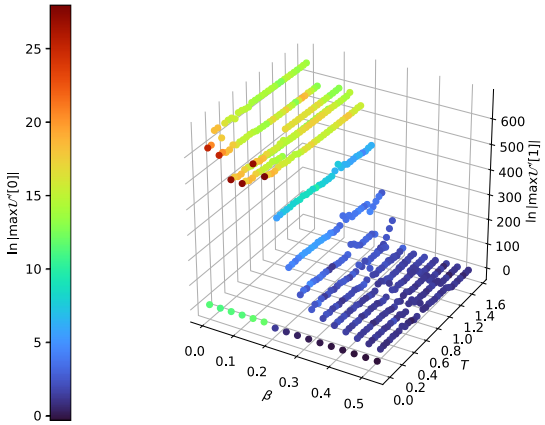

(c) Maxima of the potential for different values of β, in different points of the phase space.

Figure 10. The maximum values of the derivative of the potential at the value $\bar{\chi} = 1$ in the parameter space (a)–(c).

corresponding model, and we mention its results as an opening towards further investigations. In the same way, the above analysis does not yet provide a precise answer to the other question in the introduction, and to which we have already provided some elements of an answer in our previous articles: namely, the physically motivated position of a boundary between signal and noise. We expect the delocalization of eigenvectors to induce a mixture between the 'information' and 'noise' parts of the signal; therefore, we could, as we explained in the introduction, hope to determine a boundary in the spectrum at which we expect to find more information than noise. Here, the search for this boundary using the formalism developed in this article is a work in progress and will be the subject of future works.

We conclude this section by mentioning other results that seem to confirm the previous results. Starting with some initial conditions, we show, in figure 10, the maximal values of the derivative of the potential for two values of $\beta = 0$ and $\beta = 0.43$. According to the previous results, the values taken by the potential with vanishing β are very large, and then diverge at almost every point of the phase space. The situation is different

J. Stat. Mech. (2024) 083203

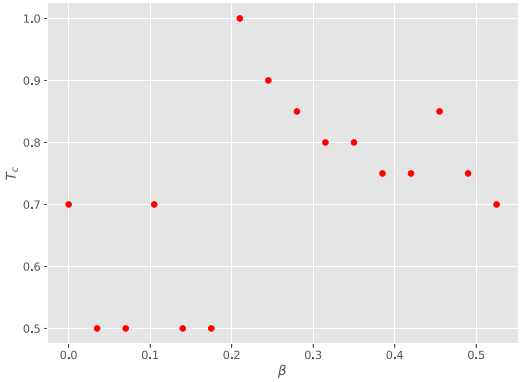

Figure 11. The behaviour of T_c as a function of the signal strength β.

for $\beta = 0.43$, where the potential takes large, though finite, values[17]. This is indeed true for almost every point in the set represented in the figure, except for a point where the potential seems to take a large value. The same phenomenon occurs for different values of β, as the last plot in figure 10 shows, using parametrization, equation (4.9), for the initial conditions. We observe that, for each value of β, a value exists for which the potential forms a 'cusp', for a given T_c value of the temperature. The value of this 'critical' temperature depends on β, and figure 11 explicitly shows its dependency. The value of the critical temperature shows the same kind of qualitative change as we had previously observed, in the vicinity of the critical value $\beta_c \simeq 0.2$. Here, again, we see that the net effect of the signal is to delay the transition point, by increasing the effective value of the critical temperature, for a given parameterization fixed in the IR.

5. Conclusion

This article continues recent work by the same authors, summarized in [30], aiming to exploit the functional RG for signal detection when the latter is hidden within highly noisy degrees of freedom (low signal-to-noise ratio). Although the authors were able to show the different behaviour of the RG as a function of the signal strength, a critical threshold for signal detection has not yet been established. However, a qualitative effect on the final phase was observed: the domain of initial conditions leading to a symmetric potential in the IR is reduced by the introduction of a deterministic signal. The symmetry-breaking process could thus be used to detect the presence of a signal. The determination of the critical threshold of the signal-to-noise ratio has yet to be solved, or solved efficiently, by current methods. Our aim is to identify not only a detection threshold, but also a characteristic spectrum scale for distinguishing a 'noisy' sector. In this article, we have considered stochastic field theory and investigated the relationship between the presence of a signal and the return to equilibrium. The net result is the existence of a transition between two clearly identified regimes: a first regime where the system never reaches equilibrium (noisy regime), and a regime where the equilibrium

[17] According to our machine limit, which does not distinguish numbers larger than 10^{308} with infinity.

J. Stat. Mech. (2024) 083203

conditions can be maintained, when the signal strength is large enough. We were thus able to give an estimate of the critical β_c value at the detection threshold, which we were unable to do in previous investigations. However, we still have a long way to go in understanding the physics of these flows. For example, we have not studied the characteristics of the potential, only its divergences; nor have we finely analysed the relevance of our approximations (LPA) when we deviate from the IR. Finally, we have not gone any further in estimating the boundary with noisy degrees of freedom; however, this question is the subject of ongoing work, and will be dealt with in the direct aftermath of this work, which should be considered as preliminary.

Acknowledgments

This project has received funding from the European Union's Horizon 2020 research and innovation program under the Marie Skłodowska-Curie Grant Agreement No 891169. This work is supported by the National Science Foundation under Cooperative Agreement PHY-2019786 (The NSF AI Institute for Artificial Intelligence and Fundamental Interactions, http://iaifi.org/). The simulations presented in this article were performed on the FactoryIA supercomputer, financially supported by the Île-De-France Regional Council, and the Engaging cluster at the MGHPCC facility. We also acknowledge the European COST Action CA22130 for the profitable exchanges on the use of the techniques in this article for data analysis.

References

[1] Li S -H and Wang L 2018 Neural network renormalization group *Phys. Rev. Lett.* **121** **260601**
[2] De Mello Koch E, De Mello Koch R and Cheng L 2020 Is deep learning a renormalization group flow? *IEEE Access* **8** 106487–505
[3] Koch-Janusz M and Ringel Z 2018 Mutual information, neural networks and the renormalization group *Nat. Phys.* **14** 578–82
[4] Mehta P and Schwab D J 2014 An exact mapping between the variational renormalization group and deep learning (arXiv:1410.3831)
[5] Bradde S and Bialek W 2017 PCA Meets RG *J. Stat. Phys.* **167** 462–75
[6] De Mello Koch A, De Mello Koch E and De Mello Koch R 2020 Why unsupervised deep networks generalize *CoRR* (arXiv:2012.03531)
[7] Koch E D M, Koch A D M, Kastanos N and Cheng L 2020 Short-sighted deep learning *Phys. Rev.* E **102** 013307
[8] Halverson J, Maiti A and Stoner K 2021 Neural networks and quantum field theory *Mach. Learn.: Sci. Technol.* **2** 035002
[9] Grosvenor K T and Jefferson R 2021 The edge of chaos: quantum field theory and deep neural networks (arXiv:2109.13247)
[10] Erbin H, Lahoche V and Ousmane Samary D 2022 Non-perturbative renormalization for the neural network-QFT correspondence *Mach. Learn. Sci. Tech.* **3** 015027
[11] Maiti A, Stoner K and Halverson J 2021 Symmetry-via-duality: invariant neural network densities from parameter-space correlators (arXiv:2106.00694)
[12] Erbin H, Lahoche V and Samary D O 2022 Renormalization in the neural network-quantum field theory correspondence Machine learning and the physical sciences *NeurIPS 2022* (arXiv:2212.11811)
[13] Banta I, Cai T, Craig N and Zhang Z 2023 Structures of neural network effective theories (arXiv:2305.02334)
[14] Grosvenor K T and Jefferson R 2022 The edge of chaos: quantum field theory and deep neural networks *SciPost Phys.* **12** 081

J. Stat. Mech. (2024) 083203

[15] Kline A G and Palmer S E 2023 Multi-relevance: coexisting but distinct notions of scale in large systems (arXiv:2305.11009)
[16] Wilson K G 1983 The renormalization group and critical phenomena *Rev. Mod. Phys.* **55** 583–600
[17] Dupuis N, Canet L, Eichhorn A, Metzner W, Pawlowski J M, Tissier M and Wschebor N 2021 The nonperturbative functional renormalization group and its applications *Phys. Rep.* **910** 1–114
[18] Zinn-Justin J 2002 *Quantum Field Theory and Critical Phenomena* (Oxford University Press)
[19] Zinn-Justin J 2019 *From Random Walks to Random Matrices* (Oxford University Press)
[20] Cotler J and Rezchikov S 2023 Renormalization group flow as optimal transport *Phys. Rev.* D **108** 025003
[21] Jolliffe I and Cadima J 2016 Principal component analysis: a review and recent developments *Phi. Trans. R. Soc.* A **374** 20150202
[22] Bény C 2018 Inferring relevant features: from QFT to PCA *Int. J. Quantum Inf.* **16** 1840012
[23] Bény C and Osborne T J 2015 The renormalization group via statistical inference *New J. Phys.* **17** 083005
[24] Meshulam L, Gauthier J L, Brody C D, Tank D W and Bialek W 2019 Coarse graining, fixed points and scaling in a large population of neurons *Phys. Rev. Lett.* **123** 17
[25] Meshulam L, Gauthier J L, Brody C D, Tank D W and Bialek W 2018 Coarse–graining and hints of scaling in a population of 1000+ neurons (arXiv:1812.11904)
[26] Lahoche V, Ousmane Samary D and Tamaazousti M 2022 Generalized scale behavior and renormalization group for data analysis *J. Stat. Mech.* **2022** 033101
[27] Lahoche V, Ousmane Samary D and Tamaazousti M 2021 Field theoretical approach for signal detection in nearly continuous positive spectra I: matricial data *Entropy* **23** 9
[28] Lahoche V, Ousmane Samary D and Tamaazousti M 2022 Signal detection in nearly continuous spectra and $\mathbb{Z}_2$-symmetry breaking *Symmetry* **14** 3
[29] Lahoche V, Ouerfelli M, Ousmane Samary D and Tamaazousti M 2021 Field theoretical approach for signal detection in nearly continuous positive spectra II: tensorial data *Entropy* **23** 7
[30] Lahoche V, Ousmane Samary D and Tamaazousti M 2022 Functional renormalization group approach for signal detection (arXiv:2201.04250)
[31] Baik J, Ben Arous G and Péché S 2005 Phase transition of the largest eigenvalue for nonnull complex sample covariance matrices *Ann. Probab.* **33** 1643–97
[32] Begdache L, Kianmehr H, Sabounchi N, Chaar M and Marhaba J 2020 Principal component analysis identifies differential gender-specific dietary patterns that may be linked to mental distress in human adults *Nutrition. Neurosci.* **23** 295–308
[33] Nobre J and Neves R 2019 Combining principal component analysis, discrete wavelet transform and XGBoost to trade in the financial markets *Expert Syst. Appl.* **125** 181–94
[34] Jaynes E T 1957 Information theory and statistical mechanics *Phys. Rev.* **106** 620–30
[35] Jaynes E T 1957 Information theory and statistical mechanics. II *Phys. Rev.* **108** 171–90
[36] Jacquin H 2016 Resummed mean-field inference for strongly coupled data *Phys. Rev.* E **94** 042118
[37] Livi R and Politi P 2017 *Nonequilibrium Statistical Physics: A Modern Perspective* (Cambridge University Press)
[38] Chen X and Bialek W 2020 Searching for long time scales without fine tuning *Phys. Rev.* E **94** 042118
[39] Hebb D O 2005 *The Organization of Behavior: A Neuropsychological Theory* (Psychology Press)
[40] Fischer K H and Hertz J A 1991 *Spin Glasses* (*Cambridge Studies in Magnetism*) (Cambridge University Press)
[41] Hohenberg P C and Halperin B I 1977 Theory of dynamic critical phenomena *Rev. Mod. Phys.* **49** 435–79
[42] Rovelli C 1993 Statistical mechanics of gravity and the thermodynamical origin of time *Class. Quantum Grav.* **10** 1549
[43] Rovelli C 1993 The statistical state of the Universe *Class. Quantum Grav.* **10** 1567
[44] Connes A and Rovelli C 1994 Von Neumann algebra automorphisms and time-thermodynamics relation in generally covariant quantum theories *Class. Quantum Grav.* **11** 2899
[45] De Dominicis C and Giardina I 2006 *Random Fields and Spin Glasses: A Field Theory Approach* (Cambridge University Press)
[46] Duclut C and Delamotte B 2017 Frequency regulators for the nonperturbative renormalization group: a general study and the model a as a benchmark *Phys. Rev.* E **95** 012107
[47] Lahoche V, Ousmane Samary D and Tamaazousti M 2023 Functional renormalization group for multilinear disordered Langevin dynamics II: revisiting the $p = 2$ spin dynamics for Wigner and Wishart ensembles *J. Phys. Commun.* **7** 055005
[48] Lahoche V, Ousmane Samary D and Ouerfelli M 2022 Functional renormalization group for multilinear disordered Langevin dynamics I: formalism and first numerical investigations at equilibrium *J. Phys. Commun.* **6** 055002
[49] Wetterich C 1991 Average action and the renormalization group equations *Nucl. Phys.* B **352** 529–84

J. Stat. Mech. (2024) 083203

[50] Wetterich C 1993 Exact evolution equation for the effective potential *Phys. Lett.* B **301** 90–94
[51] Morris T R 1994 Derivative expansion of the exact renormalization group *Phys. Lett.* B **329** 241–8
[52] Morris T R 1994 The exact renormalization group and approximate solutions *Int. J. Mod. Phys.* A **09** 2411–49
[53] Potters M and Bouchaud J -P 2020 A first course in random matrix theory: for physicists engineers and data scientists *Phys. Rev.* E **94** 042118
[54] Martin P C, Siggia E D and Rose H A 1973 Statistical dynamics of classical systems *Phys. Rev.* A **8** 423–37
[55] Aron C, Biroli G and Cugliandolo L F 2010 Symmetries of generating functionals of Langevin processes with colored multiplicative noise *J. Stat. Mech.* 11018
[56] Delamotte B 2012 An introduction to the nonperturbative renormalization group *Renormalization Group and Effective Field Theory Approaches to Many-Body Systems* (Springer) pp 49–132
[57] Canet L, Chaté H and Delamotte B 2011 General framework of the non-perturbative renormalization group for non-equilibrium steady states *J. Phys. A: Math. Theor.* **44** 495001
[58] Wilkins A, Rigopoulos G and Masoero E 2021 Functional renormalisation group for Brownian motion I: the effective equations of motion *Phys. Rev.* E **94** 042118
[59] Wilkins A, Rigopoulos G and Masoero E 2021 Functional renormalisation group for brownian motion II: accelerated dynamics in and out of equilibrium *Phys. Rev.* E **94** 042118
[60] Litim D F 2001 Optimized renormalization group flows *Phys. Rev.* D **64** 105007
[61] Zwicker D 2020 py-pde: A Python package for solving partial differential equations *J. Open Source Softw.* **5** 2158
[62] Eichhorn A 2019 An asymptotically safe guide to quantum gravity and matter *Front. Astron. Space Sci.* **5** 47

J. Stat. Mech. (2024) 083203